

Electrostatic interactions in the acid denaturation of α -lactalbumin determined by NMR

SEHO KIM¹ AND JEAN BAUM²

¹Joint Graduate Program in Biochemistry, Rutgers-UMDNJ, Piscataway, New Jersey 08854

²Department of Chemistry, Rutgers University, Piscataway, New Jersey 08855-0939

(RECEIVED December 22, 1997; ACCEPTED May 28, 1998)

Abstract

α -Lactalbumin (α -LA) undergoes a pH-dependent unfolding from the native state to a partially unfolded state (the molten globule state). To understand the role of electrostatic interactions in protein denaturation, NMR and CD pH titration experiments are performed on guinea pig α -LA. Variation of pH over the range of 7.0 to 2.0 simultaneously leads to the acid denaturation of the protein and the titration of individual ionizable groups. The pH titrations are interpreted in the context of these coupled events, and indicate that acid denaturation in α -LA is a cooperative event that is triggered by the protonation of two ionizable residues. Our NMR results suggest that the critical electrostatic interactions that contribute to the denaturation of α -LA are concentrated in the calcium binding region of the protein.

Keywords: chemical exchange; ionizable groups; NMR; pH titration; pK_a values

α -Lactalbumin (α -LA) offers an opportunity to study protein folding in the context of electrostatic interactions and metal binding (Hall & Campbell, 1986; McKenzie & White, 1991; Brew & Grobler, 1992; Sugai & Ikeguchi, 1994). Guinea pig α -LA contains 11 lysines, 4 histidines, 6 glutamic acids, and 16 aspartic acids that result in an isoelectric point of pH 4.65 (Fig. 1). α -LA isolated from milk contains an equimolar amount of bound calcium, which stabilizes the native structure, but other divalent metal ions including Mn^{2+} , Zn^{2+} , and Cu^{2+} can also bind to the protein (Kronman et al., 1981; Rao & Brew, 1989). The structure of α -LA consists of two domains, an α -helical and a β -sheet domain (Acharya et al., 1989, 1991; Pike et al., 1996), and a calcium binding loop in which two carbonyl groups corresponding to K79 and D84, and three carboxyl groups corresponding to D82, D87, and D88, act as ligands.

α -LA undergoes a pH-dependent unfolding from the native state (N-state) to the acid denatured (A-state) or molten globule state (Kuwajima et al., 1980; Sommers & Kronman, 1980). The low pH form of α -LA is an ideal model system for studies of protein folding because the “molten globule” state that it adopts at low pH has been postulated to be analogous to an early intermediate on the protein folding pathway (Kuwajima et al., 1985; Ptitsyn et al., 1990). The low pH form of α -LA has been extensively studied by CD, NMR, and other spectroscopic and physicochemical methods (Dobson, 1994; Ptitsyn, 1995; Kuwajima, 1996). It is highly het-

erogeneous, with defined secondary structure and the absence of rigid tertiary interactions (Dolgikh et al., 1981; Damaschun et al., 1986; Baum et al., 1989; Kuwajima, 1989; Ptitsyn et al., 1990; Ewbank & Creighton, 1991; Alexandrescu et al., 1993; Chyan et al., 1993; Peng & Kim, 1994; Peng et al., 1995; Schulman et al., 1995; Wu et al., 1995). Hydrogen exchange NMR studies of the acid denatured state of guinea pig and human α -LA’s have indicated that the molten globule state contains specific amides that are protected in the α -helical domain of the protein, suggesting that the α -domain forms the nucleus of the molten globule state and that the β -domain is essentially unfolded (Baum et al., 1989; Alexandrescu et al., 1993; Chyan et al., 1993; Schulman et al., 1995). In addition, unfolding studies of the molten globule state in increasing concentrations of urea show that the low pH state is not formed cooperatively (Schulman et al., 1997).

The electrostatic interactions that are important to acid denaturation in α -LA are examined using CD and NMR. NMR provides a powerful method for determining pK_a values of individual ionizable groups. Most NMR studies have been performed on proteins that do not undergo conformational changes in the pH range that is studied (Haruyama et al., 1989; Cocco et al., 1992; Forman-Kay et al., 1992; Bartik et al., 1994; Oda et al., 1994; Szyperski et al., 1994; Oliveberg et al., 1995; Qin et al., 1996). For pH denaturing proteins, such as α -LA, apomyoglobin, and barnase, a pH titration results simultaneously in the denaturation of the protein and the titration of ionizable groups (Cocco et al., 1992; Oliveberg et al., 1994, 1995). In this paper, we present a model for interpreting NMR pH titration experiments in proteins that undergo acid denaturation. Our approach allows us to relate the pH titration of individual ionizable groups to the protein denaturation, and to identify the ionizable groups that are critical to the denaturation of α -LA.

Reprint requests to: Jean Baum, Department of Chemistry, Rutgers University, Piscataway, New Jersey 08855-0939; e-mail: baum@rutchem.rutgers.edu.

Abbreviations: α -LA, α -lactalbumin; N-state, native state; A-state, acid denatured state; HSQC, heteronuclear single quantum coherence; CD, circular dichroism.

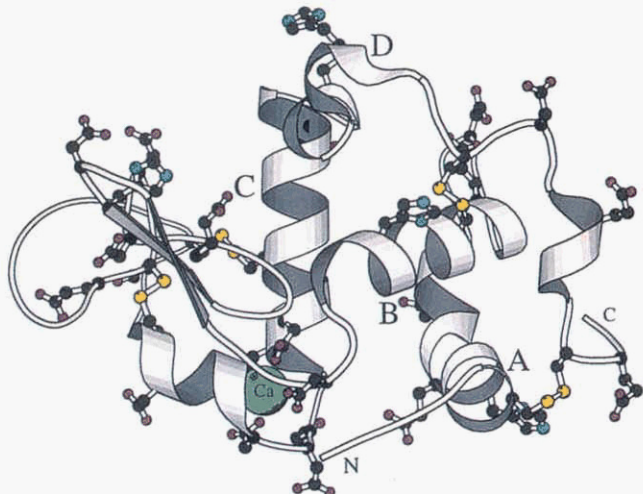


Fig. 1. X-ray crystal structure of guinea pig α -LA (Pike et al., 1996). The protein contains four α -helices located in the α -domain labeled A, B, C, and D. The side chain of ionizable D, E, and H residues are shown: H10, H32, H47, H107, E11, E25, E49, E62, E116, E121, D14, D20, D37, D46, D57, D59, D74, D78, D82, D83, D84, D87, D88, D97, D102, and D113. The structure was created by MolScript (Kraulis, 1991).

Results

NMR spectra of α -LA as a function of pH

The ^1H - ^{15}N HSQC (Bax et al., 1990) spectrum of the N-state (pH 7.0) (Fig. 2A) is typical of a folded globular protein and shows large chemical shift dispersion and well-defined resonance peaks. Assignments in the native state have been obtained by triple resonance experiments on ^{13}C and ^{15}N doubly labeled protein (Kim, 1997). The A-state spectrum (Fig. 2B), obtained at pH 2.1, is very different from the N-state spectrum, with broadened peaks and narrowed chemical shift dispersion. The small chemical shift dispersion is consistent with the partially unfolded character of the A-state, and the line broadening arises from chemical exchange on the millisecond time scale (Baum et al., 1989; pers. obs.). The HSQC spectra between pH 3.5 and 7.1 show that a significant number of ^1H - ^{15}N peaks change in chemical shift as a function of pH. The change in chemical shift of the NH atoms is attributed to the titration of neighboring ionizable groups. The protonated and deprotonated states of the ionizable residues are in fast chemical exchange on the NMR time scale, and the observed chemical shift is a weighted average of the chemical shift of the two species. The HSQC spectrum (Fig. 2C) in the transition pH region (pH 3.5) appears as a superposition of the N- and A-state spectra. The two sets of distinguishable peaks indicate that the N- and A-states are in slow conformational exchange on the NMR time scale, allowing us to measure pH titration curves for the N-state independently of those of the A-state.

Measurement of individual pK_a values by NMR

The pK_a values of individual ionizable groups are measured by NMR to determine which electrostatic interactions are critical to the denaturation of α -LA. Changes in chemical shifts of backbone ^1H and ^{15}N resonances were used to monitor pH titrations of acidic

residues. Using the crystal structure, pK_a values obtained from the NH titration curves were assigned to a specific ionizable group by determining close distances between acidic residues and amide protons (Bundi & Wüthrich, 1979; Szyperski et al., 1994; Pike et al., 1996).

NH groups are used to obtain information on the ionization constants of residues (D, E, H) in spatial proximity, and criteria for selection of the NH group that is assigned to represent a particular ionizable group is important. All distances between backbone N atoms and any ionizable groups are calculated based on the crystal structure and the closest distance varies mostly from 3 to 8 Å. A contact map (Fig. 3), between the ionizable oxygen and nitrogen atoms and the nitrogen atoms of backbone amides, was plotted to establish which ionizable groups are near a given NH. The contact map was plotted with a distance cutoff of 4 Å to show unique contacts and was also plotted with a 6 Å cutoff to indicate possible multiple contacts. The contact map, with a distance cutoff of 4 and 6 Å, indicates that a specific NH atom is always close to the ionizable atom corresponding to its own residue, and in certain cases is close to a neighboring ionizable residue as well. Long-range electrostatic effects are observed in two regions only, corresponding to the anti-parallel β -sheet of the β -domain, and the turn structure in the Ca^{2+} binding helix-turn-helix motif.

Assignment of a pH titration curve to a specific ionizable group was based on the contact map using the following criteria. In the simplest case, if there is only a single contact within 5 Å, then the ^{15}N or ^1H is unambiguously assigned to that ionizable group. In more complicated cases, if multiple contacts are found, we choose the ^{15}N or ^1H exhibited the fewest number of other neighboring ionizable groups within 5 Å. For example, the titration curve of L12 was assigned to E11 because E11 is within 5 Å of both E11 and H10, whereas L12 is close to E11 only, while the NH titration curve of D14 was assigned to represent D14 (Table 1).

Ionization constants are obtained from the analysis of the pH-dependent chemical shift changes of ^{15}N and ^1H resonances (Fig. 4). The pH titration data were divided into three groups, and representative examples are shown in Figure 4. In the first group the titration data have a simple sigmoidal shape as a function of pH (H10, E11, D14, D20, E25, H32, D37, E49, D59, E62, D74, D78, D84, D97, D113, E116, and E121); in the second group, the data show more complicated titration curves (D46, H47, D57, D83, and D88); and in the third group, the NH groups show no chemical shift change and do not titrate as a function of pH (D82 and D87).

Measurement of pK_a values was accomplished by fitting ^1H or ^{15}N pH-titration curves with a single pK_a for the simple sigmoidal shapes, or two independent pK_a 's for the more complicated titration curves (Forman-Kay et al., 1992). The single or two-p K_a fit to the experimental data and the expected interactions between ionizable groups based on the contact map of Figure 3 are consistent with one another. Although selected pH titration curves could be modulated by ionizable groups that are greater than 6 Å, the small curve fitting error for the pK_a measurements indicates that these long-range interactions are not significant. Table 1 lists the assignments for the ionizable residue, the reporter residue, and the experimental pK_a . When two independent pK_a 's were required for the fit, the residues that contributed to the fit are listed. For example, the pK_a values of D46 and H47 were obtained from a pH titration curve of H47 by a two-p K_a fit. When pK_a values were modeled by a single pK_a fit, errors were small and estimated at ± 0.1 . For two-p K_a fits, errors were larger and estimated at ± 0.4 . With the exception of two residues, all the other titration curves

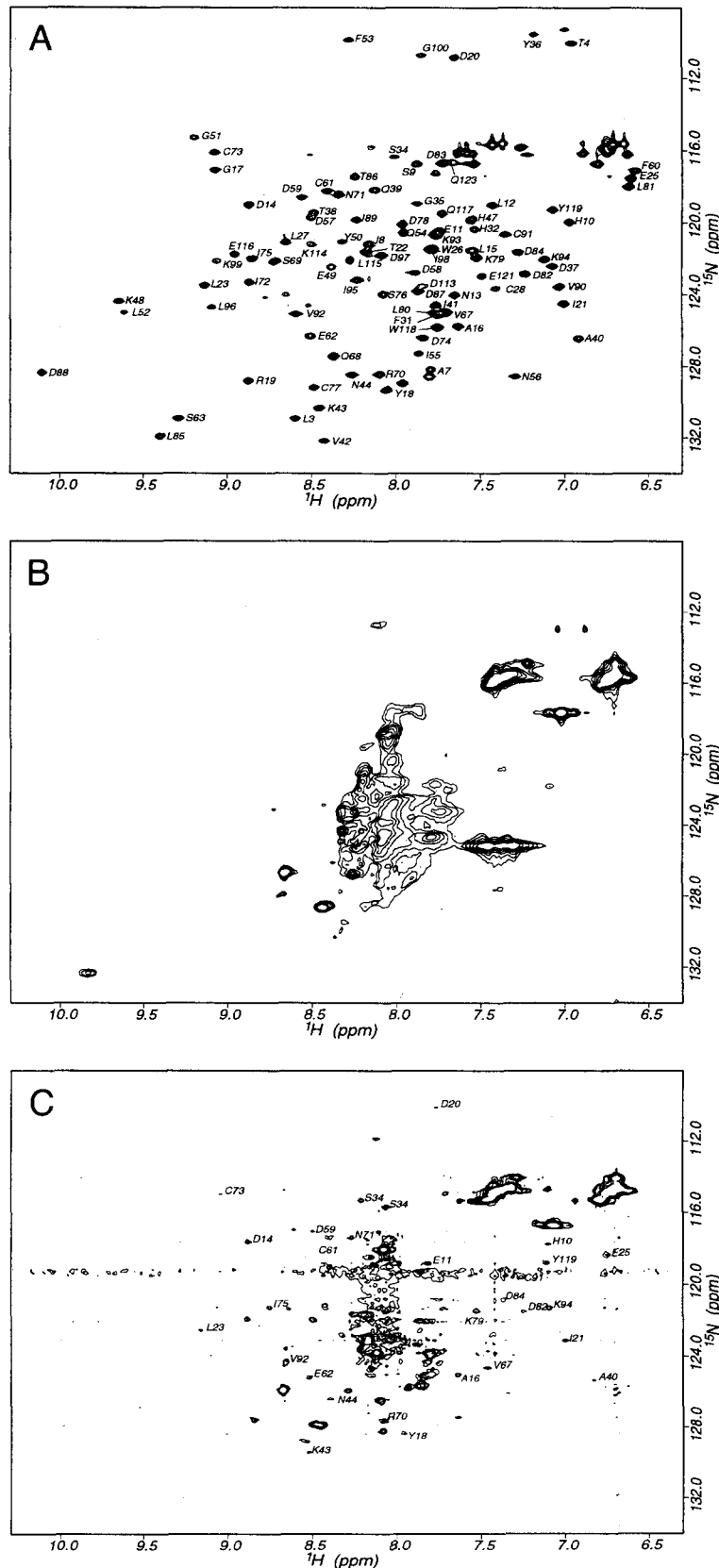


Fig. 2. ^1H - ^{15}N HSQC spectra of α -LA. The N-state spectrum (**A**) was taken at pH 7.0 and the A-state spectrum (**B**) at pH 2.1. The spectrum (**C**) near the denaturation midpoint was taken at pH 3.5 in the acid denaturation. Two sets of peaks arising from the equilibrium between the A- and N-states indicate that they are in slow conformational exchange on the NMR timescale. All spectra were acquired at 25 °C.

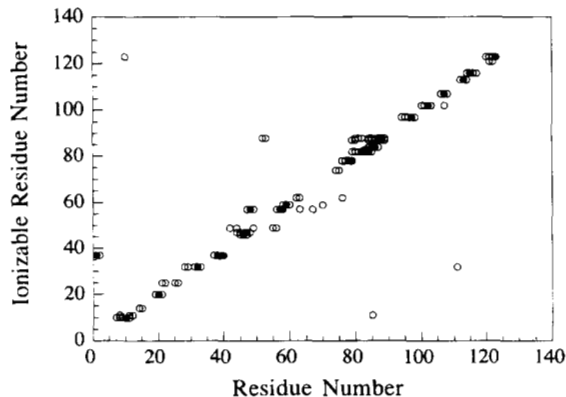


Fig. 3. Contact map between ionizable groups and amide groups in guinea pig α -LA. Distances are measured between ionizable CO or N atoms of D, E, and H residues, and backbone N atoms in the X-ray crystal structure of guinea pig α -LA. Open circles are contacts that are within 6 Å, and closed circles are within 4 Å.

Table 1. Measurement of pK_a values

Ionizable residue	Measured residue	Measured nucleus	pK_a	Two- pK_a fit ^a
H10	H10	N	6.5	
E11	L12	N	5.7	
D14	D14	N	3.9	
D20	D20	H	4.4	
E25	T22	H	5.8	
E25	T22	N	5.7	
H32	F31	H	6.0	
H32	H32	N	5.9	
H32	D88	H	5.7	H32, D88
D37	Q39	H	4.0	
D46	H47	H	4.3	D46, H47
D46	H47	N	4.3	D46, H47
H47	H47	H	6.3	H47, D46
H47	H47	N	6.9	H47, D46
H47	K58	H	6.4	H47, D57
E49	E49	N	4.4	
D57	K58	H	4.2	D57, H47
D59	F60	H	4.1	
E62	E62	N	5.1	
D74	D74	N	5.0	
D78	D78	H	3.5	
D82			ND ^b	
D83	D83	H	4.0	D83, H10, or H47
D84	D84	H	4.1	
D87			ND ^b	
D88	D88	H	3.6	D88, H32
D97	D97	N	4.1	
D102	NA ^c			
H107	NA ^c			
D113	D113	N	3.3	
E116	E116	H	4.3	
E121	E121	H	5.2	

^aWhen two independent pK_a 's were required for the fit, the residues that contributed to the fit are listed. Otherwise, a single pK_a fit was used.

^bNot determined.

^cNot assigned.

could be well fit with a single or two independent pK_a values. The pK_a values of 3 histidines, 6 glutamic acids, and 13 aspartic acids are determined (Table 1). The pK_a values for D82 and D87 could not be obtained, as these residues showed no chemical shift change as a function of pH. In addition, there are two unassigned ionizable residues (D102 and H107).

CD Denaturation profile of α -LA as a function of pH

α -LA undergoes a conformational transition from the N-state to the A-state as a function of pH (Fig. 5). The denaturation was monitored by CD by measuring the ellipticity at 280 nm as a function of pH. The denaturation profile is sharp and occurs in the range of pH 3.0 to 5.0.

A model of acid denaturation of α -LA, which simultaneously includes the denaturation to the A-state and the protonation of ionizable residues, is presented in Figure 6 (Tanford, 1968, 1970; Anderson et al., 1990; Oliveberg et al., 1995). It is assumed that at least four states are in equilibrium with one another (Fig. 6) and that n cooperative protonation sites are required for denaturation to occur. The equilibrium states are the deprotonated N-state (N^{n-}), the protonated N-state (N^{nH}), the protonated A-state (A^{nH}), and the deprotonated A-state (A^{n-}), assuming n cooperative protonation sites. The respective equilibrium constant between the N^{n-} state and the N^{nH} state is K_N , between A^{n-} and A^{nH} is K_A , between N^{n-} and A^{n-} is K_u , and between N^{nH} and A^{nH} is K_p . The calcium binding dissociation constant (K_d) is not explicitly included in the model, but is directly related to K_u or K_p by $K_d = K_u[\text{Ca}^{2+}]$ or $K_p[\text{Ca}^{2+}]$, assuming that the N-state is Ca^{2+} bound and the A-state is Ca^{2+} free. The N^{n-} and N^{nH} states are indicated as being in fast chemical exchange on the NMR time scale because of the continuous chemical shift changes in the pH titration, and the N^{nH} and A^{nH} states are in slow conformational exchange because the denaturation midpoint shows two sets of independent peaks that arise from the N- and A-states.

The number of cooperative protonation sites, n , and the equilibrium constants that define the acid denaturation can be obtained by fitting the CD curve (Fig. 5) to the equations that describe acid denaturation (Fig. 6). A minimized solution is obtained and values for the equilibrium constants, pK_{a_N} , pK_{a_A} , K_p , and for n , the number of cooperative protonation sites, are derived from the fit (curve-fitting errors are within 2%). The number of cooperative protonation sites, n , required for denaturation of α -LA is small, and equal to 2.14. We assume, therefore, that the cooperative protonation of two residues is critical to triggering acid denaturation. For this group of critical residues, the equilibrium constant, K_p , between the protonated N-state (N^{nH}) and the protonated A-state (A^{nH}) is large ($K_p = 164$), implying that the N^{nH} population is negligible during the denaturation process and that the population is shifted toward the A-state.

Average pK_a values in the N- and A-states, for the two cooperative protonation sites corresponding to n , can be obtained from the fit of the CD data to the model in Figure 6. The average pK_a value of the two critical residues is 2.84 in the N-state ($pK_{a_N} = 2.84$) and 4.76 ($pK_{a_A} = 4.76$) in the A-state. It is interesting to note that the pK_a values of the critical residues involved in the denaturation of the protein ($pK_a = 2.84$) do not correspond to the pH midpoint of the denaturation curve (pH = 3.8) (Yang & Honig, 1993). The equilibria between the native and denatured states (Fig. 6) imply that the pK_a values of both of these states are important in specifying the pH at which denaturation occurs, and

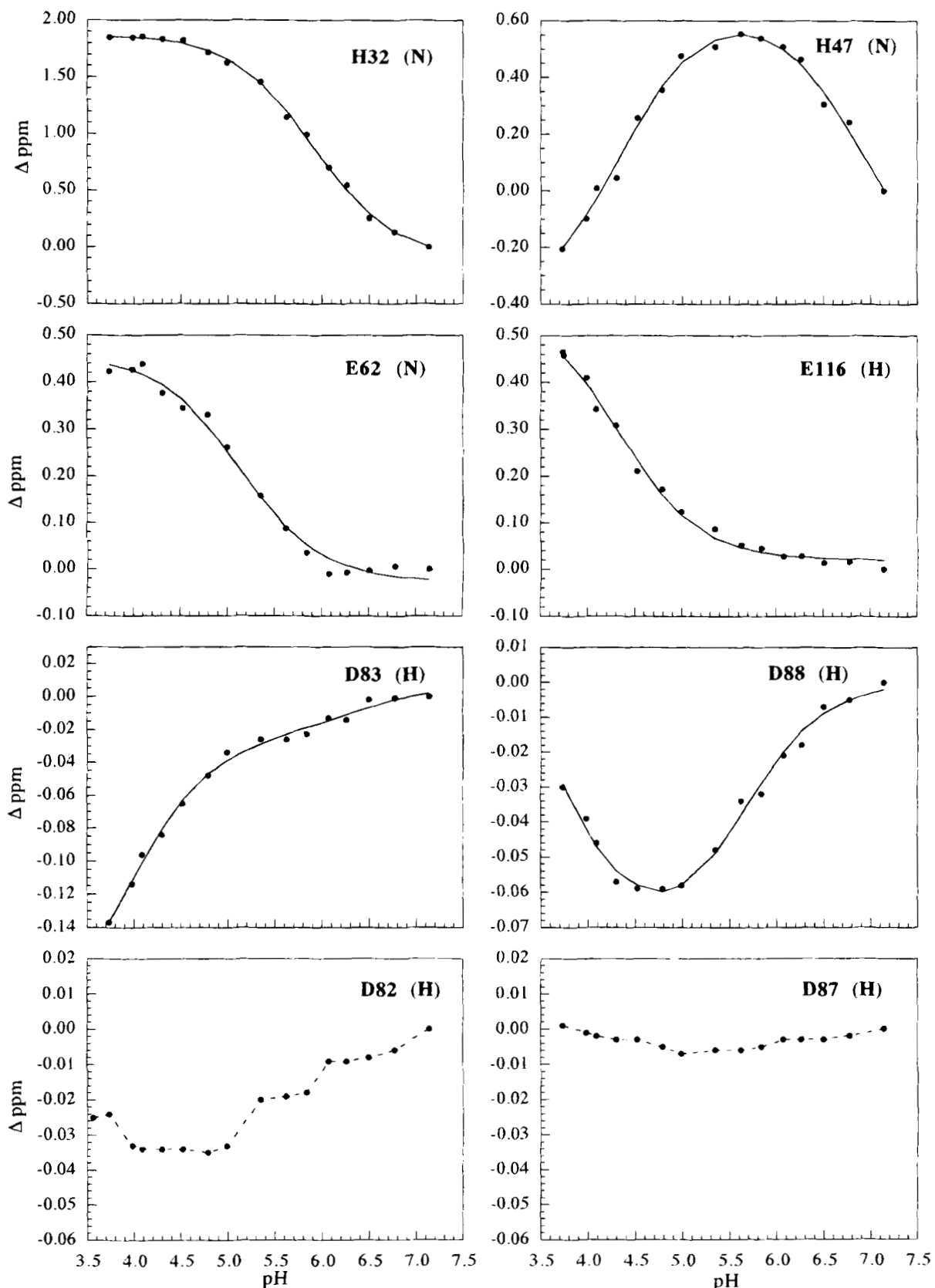


Fig. 4. pH titration curves. ^1H or ^{15}N chemical shift changes (Δppm) are plotted as a function of pH (pH 7.1 to 3.5). To determine pK_a values, pH titration curves were simulated with one or two independent pK_a 's. All ionizable residues, except for D82 and D87, showed titration curves for which pK_a values could be obtained. The titration curves of D82 and D87 are essentially flat over the pH range, although D82 shows a small shift from pH 7.0 to 5.0 that is attributed to H10 or H47.

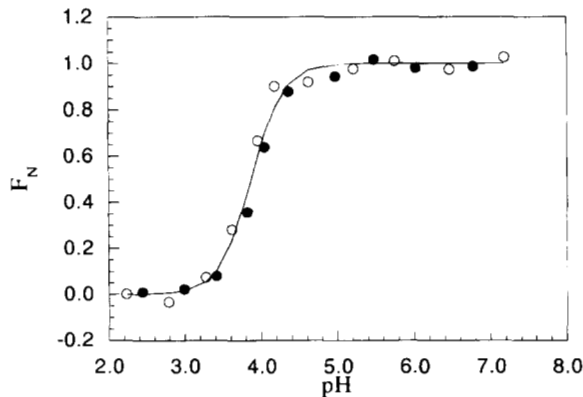


Fig. 5. Acid denaturation monitored by CD at 280 nm. Titrations from pH 7.0 to pH 2.0 (open circles) and from pH 2.0 to pH 7.0 (closed circles) were done reversibly at 25 °C. The fraction of the N-state (F_N) decreases sharply as a function of pH. The denaturation midpoint is pH 3.8.

that the pK_a values of the native state alone are not sufficient to predict the midpoint of the acid denaturation.

The pH dependence of the Ca^{2+} binding constant can be determined from the pH denaturation curve, because the key ionizable groups that induce acid denaturation are Ca^{2+} binding ligands. K_u in the acid denaturation is related to the Ca^{2+} binding constant of α -LA in the N-state, and K_p is related to the Ca^{2+} binding constant in the A-state (Fig. 6). K_u and K_p have the following relationship with pK_{a_N} and pK_{a_A} :

$$\frac{K_u}{K_p} = \frac{K_A}{K_N} = \frac{10^{n(\text{pH} - pK_{a_A})}}{10^{n(\text{pH} - pK_{a_N})}}.$$

The ratio of K_u and K_p is 7.8×10^{-5} from CD data. This indicates that Ca^{2+} is bound 10^4 – 10^5 times more strongly in the native state than in the A-state. The measured Ca^{2+} binding constants of α -LA range from 10^6 – 10^9 M^{-1} , depending on the method of measurement and the species (Segawa & Sugai, 1983; Kronman, 1989). The N-state binding constants, together with the ratio of K_u/K_p , suggest that the A-state binds Ca^{2+} very weakly, and confirms previous observations (Permyakov et al., 1981, 1985; Kronman, 1989). In addition, it has been shown that the denaturation midpoint and the denaturation cooperativity depend on the Ca^{2+} con-

centration in the media (Permyakov et al., 1985). The pH dependence of the Ca^{2+} binding constants will mirror the pH denaturation curve.

Interpretation of NMR pH titration curves for residues involved in denaturation

The pH titration curves of the residues that are critical to acid denaturation depend on the equilibrium constants shown in Figure 6. The NMR pH titration curves for the N-state are defined by the population of the N^{n-} and $\text{N}^{n\text{H}}$ states, which are determined by the equilibrium constants K_p , K_u , and the pK_{a_N} of the titratable group. From the fit of the acid denaturation curve shown in Figure 5, K_p is large (>150), implying that the population of $\text{N}^{n\text{H}}$ will be very small for the critical residues involved in denaturation. Therefore, the NMR pH titration curves of the critical residues will reflect primarily the population of the N^{n-} state, and no chemical shift change will be expected as a function of pH for these key residues. Examination of the data in Table 1 indicates that two residues do not show chemical shift changes as a function of pH and have flat pH titration curves below pH 5.5. These residues correspond to D82 and D87 and are believed to be critical to acid denaturation in α -LA. The chemical shift changes between pH 7.0 and pH 5.5 seen for D82 and D83 result from the neighboring titration of H47 or H10 and do not reflect the titration of the Asp groups. Because the titration curve is flat for D82 and D87, the pK_a values cannot be measured directly from the NMR pH titration experiments.

The fact that the NMR data suggest that there are two residues that are critical to acid denaturation is internally consistent with the fact that n , the number of cooperative protonation sites involved in denaturation by CD, is also two. Therefore, the two residues, D82 and D87, which are believed to be critical to acid denaturation based on the NMR data, are equated with the two cooperative protonation sites in the CD denaturation profile. This suggests that the average pK_a values of D82 and D87 are the average pK_a values (2.84 in the N-state and 4.76 in the A-state) of the two cooperative binding sites calculated from the CD denaturation profile.

Discussion

NMR and CD pH titration experiments were performed on guinea pig α -LA to determine the electrostatic interactions that are critical to acid denaturation. Variation of pH over the range of 7.0 to 2.0 leads simultaneously to titration of individual ionizable groups and to the acid denaturation of the protein. NMR pH titration profiles were obtained for 24 residues; of these, 22 titrations resulted in the determination of pK_a values and two residues, D82 and D87, showed a flat pH titration curve over the pH range that was examined. Curve fitting to the CD denaturation profile of α -LA as a function of pH indicated that cooperativity for denaturation from the native state to the acid unfolded state is on the order of 2, and that the population of the protonated form for residues that are critical to denaturation is essentially negligible. Therefore, protonation of residues D82 and D87, both of which have flat titration curves as a function of pH, is critical to acid denaturation. Examination of the crystal structure shows that the carboxyl groups of D82 and D87 form ligands for Ca^{2+} binding. The Ca^{2+} binding motif of α -LA is composed of the C helix from the α -domain and a β -helix from the β -domain, with the ligands D87 and D82 located in the two separate domains (Fig. 7).

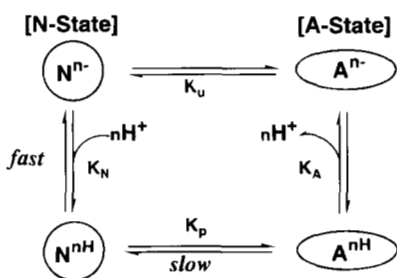


Fig. 6. Mechanism of acid denaturation. In acid denaturation, at least four states are in equilibrium: N^{n-} (deprotonated N-state), $\text{N}^{n\text{H}}$ (protonated N-state), $\text{A}^{n\text{H}}$ (protonated A-state), and A^{n-} (deprotonated A-state), assuming n protonation sites. The related equilibrium constants are $K_N = [\text{N}^{n-}]/[\text{N}^{n\text{H}}]$, $K_A = [\text{A}^{n-}]/[\text{A}^{n\text{H}}]$, $K_p = [\text{A}^{n\text{H}}]/[\text{N}^{n\text{H}}]$, and $K_u = [\text{A}^{n-}]/[\text{N}^{n-}]$.

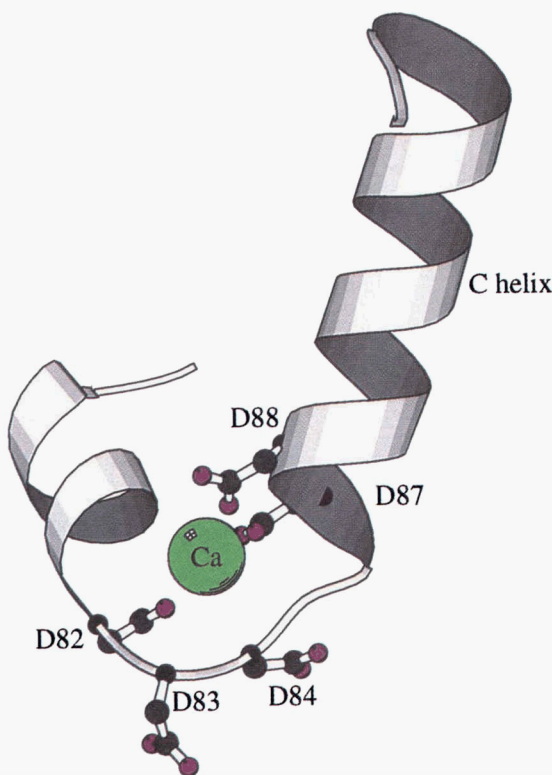


Fig. 7. Ca^{2+} binding site of guinea-pig α -LA (Pike et al., 1996). The helix-turn-helix motif of the Ca^{2+} binding site consists of a 3_{10} helix in the β domain, a Ca^{2+} binding loop, and the C helix from the α domain. The calcium binding loop contains five aspartic acids, and the ionizable groups of D82, D87, and D88 are involved in the Ca^{2+} binding. The carboxyl groups of D83 and D84 are not ligands. D82 and D87 are key residues that protonation triggers the acid denaturation. The structure was plotted using MolScript (Kraulis, 1991).

Given the pH titration experiments described here, and the energetics of denaturation obtained by Privalov (Griko et al., 1994), it is interesting to speculate on the electrostatic interactions that are critical to acid denaturation and on the factors that stabilize the native state of the protein. Privalov has measured the excess heat capacity function of holo α -LA as a function of pH and analyzed the data in terms of a hierarchical cooperative model (Griko et al., 1994). At pH values greater than five, the transition is close to two state, and thermal denaturation results in complete unfolding with no significant population of compact denatured molecules. These data imply that the protonation of residues at pH values greater than 5.0 do not contribute to the formation of the compact denatured state. Below pH 4.2, the transition results in a progressively higher proportion of compact denatured molecules, and the free energy of unfolding at pH 4.2 corresponds to ~ 17 kJ/mol, given Privalov's enthalpy and entropy values (Griko et al., 1994). Table 1 shows that the aspartic acids in α -LA titrate in the pH range for which the free energy of unfolding changes as a function of pH, suggesting that protonation of some, or all, of the aspartic acids contribute to the denaturation process.

The lowest of the experimentally determined pK_a 's in the native state arises from residues D82 and D87 ($pK_{a_N} = 2.84$, calculated from the pH denaturation curve) and is shifted by 1.9 units relative to the average pK_a value in the A-state ($pK_{a_A} = 4.76$). The signif-

icant difference in the pK_a values of the native and acid unfolded states suggests that the largest contribution to the stability of the native state derives from the strong stabilization of the charged form of D82 and D87 with the calcium. It is difficult to estimate the energetic contributions from the protonation of the remaining aspartic acids to the stabilization of the native state, because the pK_a values in the acid unfolded state are not known. However, based on the large pK_a difference between the native and acid unfolded states of residues D82 and D87, and the more uniform pK_a values of the remaining aspartic acids, it is reasonable to propose that electrostatic interactions of the remaining aspartic acids are a secondary contribution to the stabilization of the native state. Of particular interest is D88, whose carboxyl group acts as a ligand for Ca^{2+} binding along with D82 and D87. Our data indicate that protonation of D88 does not trigger denaturation to the acid unfolded state. Although protonation of D88 may result in a small change in the free energy of unfolding, the charge balance of the Ca^{2+} is maintained by the ionized form of D82 and D87. The pK_a shifts described here are consistent with previous potentiometric titrations in which abnormally titrating carboxyl groups were observed in acid denaturation (Robbins et al., 1967; Kita et al., 1976; Kuwajima et al., 1981).

α -LA and lysozyme are very similar proteins in terms of their amino acid sequence and global folds, but they differ in ligand binding properties and folding behavior (Acharya et al., 1994; Sugai & Ikeguchi, 1994). α -LA undergoes a pH-dependent conformational change, whereas lysozyme conforms more closely to a two-state model, and has no well-defined equilibrium intermediate state (Kuwajima et al., 1985). In lysozyme many of the ionizable groups have significantly shifted pK_a values relative to the model compounds (Bartik et al., 1994), whereas the pK_a values in α -LA appear to be more uniform. It is, however, difficult to make a direct comparison between the two proteins because the pK_a values in the A-state are not known for α -LA.

With regard to their unfolding behavior, it appears an important difference between α -LA and lysosomes arises from their calcium binding properties (Haezerbrouck et al., 1993; Nitta et al., 1993; Van Dael et al., 1993; Griko et al., 1995; Pardon et al., 1995; Wu et al., 1996; Kuhlman et al., 1997). Recently, the functional role of the calcium binding residues in α -LA was investigated by site-directed mutagenesis (Anderson et al., 1997). The mutations provide information about whether the different aspartic acid ligands are required for calcium binding, and are complementary to our data, which report on the role of charge interactions, between the aspartic acids and the Ca^{2+} , in triggering denaturation. Taken together with previous work, our results suggest that the electrostatic interactions between the α - and β -domains, mediated by calcium binding to D82 and D87, are important to the stability of the native state, and that the loss of these interactions results in the denaturation to the A-state (Wu et al., 1996; Kuhlman et al., 1997).

Materials and methods

Preparation of sample

^{15}N -Labeled guinea pig α -LA (M90V mutant) was produced using an *E. coli* expression system (Kim et al., 1997).

NMR spectroscopy

For acid denaturation, a protein solution (0.3 mM) was prepared in 10 mM sodium phosphate buffer at pH 7.0, 1 mM CaCl_2 , and 10%

D_2O . Excess Ca^{2+} was used because α -LA is a calcium binding protein. pH titrations were performed reversibly. Titrations from pH 7.1 to 2.1 and from pH 2.1 to 7.1 were done with 0.5 pH unit intervals and the pH was measured at each point. At each pH, an 1H - ^{15}N HSQC (heteronuclear single quantum coherence) (Bax et al., 1990) spectrum was acquired with 1,024 complex points (t_2 , 1H) by 128 complex points (t_1 , ^{15}N) at 25 °C using a Varian Unity_{plus} 500 MHz NMR. The spectral widths were 7,000 Hz in the 1H and 1,500 Hz in the ^{15}N dimensions. NMR data were processed using the Felix package (Molecular Simulations Inc., San Diego, California).

CD spectroscopy

α -LA solutions (0.02 mM) were prepared in 10 mM sodium phosphate buffer pH 7.0 and 1 mM $CaCl_2$. The protein solution was titrated in the same way as in the NMR experiment. At each pH, the CD ellipticity was measured at 280 nm with a 10-mm cell, and at 222 nm with a 1-mm cell on an AVIV model 60DS CD spectrometer at 25 °C.

Measurement of pK_a values

To assign an NH titration curve to the protonation of a specific ionizable group, distances and contacts between NH groups and ionizable groups were examined using the X-ray crystal structure of guinea pig α -LA (Pike et al., 1996). NH titration curves were assigned to an ionizable group (Bundi & Wüthrich, 1979; Szyperski et al., 1994), and pK_a values were obtained by simulating the pH titration data with the Henderson-Hasselbalch equation with one or two pK_a 's assumed to be independent (Forman-Kay et al., 1992). Experimental data were fit to an ideal titration curve which describes the titration of each ionizable group. For one pK_a value, the observed chemical shift (δ) was simulated by the pK_a , δ (chemical shift of the basic form), and δ_a (chemical shift of the acidic form) using Equation 1.

$$\delta = \frac{\delta_b 10^{(pH-pK_a)} + \delta_a}{10^{(pH-pK_a)} + 1}. \quad (1)$$

For two pK_a values, the observed chemical shift (δ) was simulated by pK_{a1} , pK_{a2} , δ_b , δ_a , and δ_i (chemical shift of the intermediate form) using Equation 2:

$$\delta = \frac{\delta_b 10^{(2pH-pK_{a1}-pK_{a2})} + \delta_i 10^{(pH-pK_{a2})} + \delta_a}{10^{(2pH-pK_{a1}-pK_{a2})} + 10^{(pH-pK_{a2})} + 1}. \quad (2)$$

Modeling of acid denaturation

The acid denaturation curves obtained by CD were modeled by the mechanism of acid denaturation shown in Figure 6. Each equilibrium constant is defined as follows:

$$\begin{aligned} K_N &= \frac{[N^{n-}]}{[N^{nH}]} = 10^{n(pH-pK_{a_N})} \\ K_A &= \frac{[A^{n-}]}{[A^{nH}]} = 10^{n(pH-pK_{a_A})} \\ K_p &= \frac{[A^{nH}]}{[N^{nH}]} \\ K_u &= \frac{[A^{n-}]}{[N^{n-}]} = \frac{K_p K_A}{K_N} \end{aligned} \quad (3)$$

where n is the number of cooperative protonation sites required for denaturation, and pK_{a_N} and pK_{a_A} are average pK_a values in the N- and A-states over these n protonation sites. K_p and K_u are equilibrium constants in the protonated and unprotonated states. F_N , represented in Figure 5, is a sum of fractions of the native states (N^{n-} and N^{nH}) and is a function of n , pK_{a_N} , pK_{a_A} , and K_p .

$$F_N = \frac{10^{n(pH-pK_{a_N})} + 1}{K_p(10^{n(pH-pK_{a_A})} + 1) + 10^{n(pH-pK_{a_N})} + 1}. \quad (4)$$

The experimental F_N and pH are used as input and the equation was fit using the Levenberg-Marquardt method (Press et al., 1992). Values of n , pK_{a_N} , pK_{a_A} , and K_p were obtained from the fit. It is important to note that pK_{a_N} and pK_{a_A} , obtained from the curve fitting, represent average pK_a values over n cooperative titrating groups only. The curve fitting error was small, on the order of 2%.

Electronic supplementary material

NMR pH titration curves for H10, L12, D14, D20, T22, Q39, H47, E49, K58, F60, D74, D78, D84, D97, D113, and E121 were also modeled to obtain pK_a values listed in Table 1.

Acknowledgments

This work was supported by NIH grant GM45302. J.B. is a Camille and Henry Dreyfus Teacher-Scholar. We would like to thank Professors Stephen Anderson and Alan Goldman for helpful discussions.

References

- Acharya KR, Ren J, Stuart DI, Phillips DC, Fenna RE. 1991. Crystal structure of human α -lactalbumin at 1.7 Å resolution. *J Mol Biol* 221:571–581.
- Acharya KR, Stuart DI, Phillips DC, McKenzie HA, Teahan CG. 1994. Models of the three-dimensional structures of echidna, horse, and pigeon lysozymes: Calcium-binding lysozymes and their relationship with α -lactalbumins. *J Protein Chem* 13:569–584.
- Acharya KR, Stuart DI, Walker NPC, Lewis M, Phillips DC. 1989. Refined structure of baboon α -lactalbumin at 1.7 Å resolution. *J Mol Biol* 208:99–127.
- Alexandrescu AT, Evans PA, Pitkeathly M, Baum J, Dobson CM. 1993. Structure and dynamics of the acid-denatured molten globule state of α -lactalbumin: A two-dimensional NMR study. *Biochemistry* 32:1707–1718.
- Anderson DE, Becktel WJ, Dahlquist FW. 1990. pH-induced denaturation of proteins: A single salt bridge contributes 3–5 kcal/mol to the free energy of folding of T4 lysozyme. *Biochemistry* 29:2403–2408.
- Anderson PJ, Brooks CL, Berliner LJ. 1997. Functional identification of calcium binding residues in bovine α -lactalbumin. *Biochemistry* 36:11648–11654.
- Bartik K, Redfield C, Dobson CM. 1994. Measurement of the individual pK_a values of acidic residues of hen and turkey lysozymes by two-dimensional 1H NMR. *Biophys J* 66:1180–1184.
- Baum J, Dobson CM, Evans PA, Hanley C. 1989. Characterization of a partly folded protein by NMR methods: Studies on the molten globule state of guinea pig α -lactalbumin. *Biochemistry* 28:7–13.
- Bax A, Ikura M, Kay LE, Torchia DA, Tschudin R. 1990. Comparison of different mode of two-dimensional reverse-correlation NMR for the study of proteins. *J Magn Res* 86:304–318.
- Brew K, Grobler JA. 1992. α -Lactalbumin. In: Fox PF, ed. *Advanced dairy chemistry*. London, UK: Elsevier Science Publishers. pp 191–229.
- Bundi A, Wüthrich K. 1979. Use of amide 1H -NMR titration shifts for studies of polypeptide conformation. *Biopolymers* 18:299–311.
- Chyan C, Wormall C, Dobson CM, Evans PA, Baum J. 1993. Structure and stability of the molten globule state of guinea-pig α -lactalbumin: A hydrogen exchange study. *Biochemistry* 32:5681–5691.
- Cocco MJ, Kao Y, Phillips AT, Lecomte JTJ. 1992. Structural comparison of apomyoglobin and metaqueomyoglobin: pH titration of histidines by NMR spectroscopy. *Biochemistry* 31:6481–6491.

- Damaschun G, Gernat C, Damaschun H, Bychkova VE, Ptitsyn OB. 1986. Comparison of intramolecular packing of a protein in native and 'molten globule' states. *Int J Biol Macromol* 8:226–230.
- Dobson CM. 1994. Solid evidence for molten globules. *Curr Biol* 4:636–640.
- Dolgikh DA, Gilmanish RI, Brazhnikov EV, Bychkova VE, Semisotnov GV, Venyaminov SY, Ptitsyn OB. 1981. α -Lactalbumin: Compact state with fluctuating tertiary structure? *FEBS Lett* 136:311–315.
- Ewbank JJ, Creighton TE. 1991. The molten globule protein conformation probed by disulfide bonds. *Nature* 350:518–520.
- Forman-Kay JD, Clore GM, Gronenborn AM. 1992. Relationship between electrostatics and redox function in human thioredoxin: Characterization of pH titration shifts using two-dimensional homo- and heteronuclear NMR. *Biochemistry* 31:3442–3452.
- Griko YV, Freire E, Privalov PL. 1994. Energetics of the α -lactalbumin states: A calorimetric and statistical thermodynamic study. *Biochemistry* 33:1889–1899.
- Griko YV, Freire E, Privalov G, Van Dael H, Privalov PL. 1995. The unfolding thermodynamics of c-type lysozymes: A calorimetric study of the heat denaturation of equine lysozyme. *J Mol Biol* 252:447–459.
- Haezebrouck P, De Baetselier A, Joniau M, Van Dael H, Rosenberg S, Hansens I. 1993. Stability effects associated with the introduction of a partial and a complete Ca^{2+} -binding site into human lysozyme. *Protein Eng* 6:643–649.
- Hall L, Campbell PN. 1986. α -Lactalbumin and related proteins: A versatile gene family with an interesting parentage. *Essays Biochem* 22:1–26.
- Haruyama H, Qian Y, Wüthrich K. 1989. Static and transient hydrogen-bonding interactions in recombinant desulfatohirudin studied by ^1H nuclear magnetic resonance measurements of amide proton exchange rates and pH-dependent chemical shifts. *Biochemistry* 28:4312–4317.
- Kim S. 1997. Expression, NMR assignments, and acid denaturation of guinea pig α -lactalbumin [Ph.D. Thesis]. New Brunswick, NJ: Rutgers University.
- Kim S, Baum J, Anderson S. 1997. Production of correctly folded recombinant [^{13}C , ^{15}N]-enriched guinea pig [Val90]- α -lactalbumin. *Protein Eng* 10:455–462.
- Kita N, Kuwajima K, Nitta K, Sugai S. 1976. Equilibrium and kinetics of the unfolding of α -lactalbumin by guanidine hydrochloride (II). *Biochim Biophys Acta* 427:350–358.
- Kraulis PJ. 1991. MOLSCRIPT: A program to produce both detailed and schematic plots of protein structures. *J Appl Crystallogr* 24:946–950.
- Kronman MJ. 1989. Metal-ion binding and the molecular conformational properties of α -lactalbumin. *CRC Crit Rev Biochem Mol Biol* 24:565–667.
- Kronman M, Sinha SK, Brew K. 1981. Characteristics of the binding of Ca^{2+} and other divalent metal ions to bovine α -lactalbumin. *J Biol Chem* 256:8582–8587.
- Kuhlman B, Boice JA, Wu W, Fairman R, Raleigh DP. 1997. Calcium binding peptides from α -lactalbumin: Implications for protein folding and stability. *Biochemistry* 36:4607–4615.
- Kuwajima K. 1989. The molten globule state as a clue for understanding the folding and cooperativity of globular-protein structure. *Proteins Struct Funct Genet* 6:87–103.
- Kuwajima K. 1996. The molten globule state of α -lactalbumin. *FASEB J* 10:102–109.
- Kuwajima K, Hiraoka Y, Ikeguchi M, Sugai S. 1985. Comparison of the transient folding intermediates in lysozyme and α -lactalbumin. *Biochemistry* 24:874–881.
- Kuwajima K, Nitta K, Sugai S. 1980. Intramolecular perturbation of tryptophans induced by the protonation of ionizable groups in goat α -lactalbumin. *Biochim Biophys Acta* 623:389–401.
- Kuwajima K, Ogawa Y, Sugai S. 1981. Role of the interaction between ionizable groups in the folding of bovine α -lactalbumin. *J Biochem* 89:759–770.
- McKenzie HA, White JFH. 1991. Lysozyme and α -lactalbumin. *Adv Protein Chem* 41:173–315.
- Nitta K, Tsuge H, Iwamoto H. 1993. Comparative study of the stability of the folding intermediates of the calcium-binding lysozymes. *Int J Peptide Protein Res* 41:118–123.
- Oda Y, Yamazaki T, Nagayama K, Kanaya S, Kuroda Y, Nakamura H. 1994. Individual ionization constants of all the carboxyl groups in ribonuclease HI from *Escherichia coli* determined by NMR. *Biochemistry* 33:5275–5284.
- Oliveberg M, Arcus VL, Fersht AR. 1995. pK_A values of carboxyl groups in the native and denatured states of barnase: The pK_A values of the denatured state are on average 0.4 units lower than those of model compounds. *Biochemistry* 34:9424–9433.
- Oliveberg M, Vuilleumier S, Fersht AR. 1994. Thermodynamic study of the acid denaturation of barnase and its dependence on ionic strength: Evidence for residual electrostatic interactions in the acid/thermally denatured state. *Biochemistry* 33:8826–8832.
- Pardon E, Haezebrouck P, De Baetselier A, Hooke SD, Fancourt KT, Doesmet J, Dobson CM, Van Dael H, Joniau M. 1995. A Ca^{2+} -binding chimera of human lysozyme and bovine α -lactalbumin that can form a molten globule. *J Biol Chem* 270:10514–10524.
- Peng Z, Kim PS. 1994. A protein dissection study of a molten globule. *Biochemistry* 33:2136–2141.
- Peng Z, Wu LC, Kim PS. 1995. Local structural preferences in the α -lactalbumin molten globule. *Biochemistry* 34:3248–3252.
- Permyakov EA, Morozova LA, Burstein EA. 1985. Cation binding effects on the pH, thermal and urea denaturation transitions in α -lactalbumin. *Biophys Chem* 21:21–31.
- Permyakov EA, Yarmolenko VV, Kalinichenko LP, Morozova LA, Burstein EA. 1981. Calcium binding to α -lactalbumin: Structural rearrangement and association constant evaluation by means of intrinsic protein fluorescence changes. *Biochem Biophys Res Commun* 100:191–197.
- Pike ACW, Brew K, Acharya KR. 1996. Crystal structures of guinea-pig, goat, and bovine α -lactalbumin highlight the enhanced conformational flexibility of regions that are significant for its action in lactose synthase. *Structure* 4:691–703.
- Press WH, Teukolsky SA, Vetterling WT, Flannery BP. 1992. *Numerical recipes in C*, 2nd ed. New York: Cambridge University Press.
- Ptitsyn OB. 1995. Structure of folding intermediates. *Curr Opin Struct Biol* 5:74–78.
- Ptitsyn OB, Pain RH, Semisotnov GV, Zerovnik E, Razgulaga OI. 1990. Evidence for a molten globule state as a general intermediate in protein folding. *FEBS Lett* 262:20–24.
- Qin J, Clore GM, Gronenborn AM. 1996. Ionization equilibria for side-chain carboxyl groups in oxidized and reduced human thioredoxin and in the complex with its target peptide from the transcription factor NF κ B. *Biochemistry* 35:7–13.
- Rao KR, Brew K. 1989. Calcium regulates folding and disulfide-bond formation in α -lactalbumin. *Biochem Biophys Res Commun* 163:1390–1396.
- Robbins FM, Andreotti RE, Holmes LG, Kronman MJ. 1967. Inter- and intramolecular interactions of α -lactalbumin VII. The hydrogen ion titration curve of α -lactalbumin. *Biochim Biophys Acta* 133:33–45.
- Schulman BA, Kim PS, Dobson CM, Redfield C. 1997. A residue-specific NMR view of the non-cooperative unfolding of a molten globule. *Nat Struct Biol* 4:630–634.
- Schulman BA, Redfield C, Peng Z, Dobson CM, Kim PS. 1995. Different subdomains are most protected from hydrogen exchange in the molten globule and native states of human α -lactalbumin. *J Mol Biol* 253:651–657.
- Segawa T, Sugai S. 1983. Interactions of divalent metal ions with bovine, human, and goat α -lactalbumins. *J Biochem* 93:1321–1328.
- Sommers PB, Kronman MJ. 1980. Comparative fluorescence properties of bovine, goat, human, and guinea pig α -lactalbumin. Characterization of the environments of individual tryptophan residues in partly folded conformers. *Biophys Chem* 11:217–232.
- Sugai S, Ikeguchi M. 1994. Conformational comparison between α -lactalbumin and lysozyme. *Adv Biophys* 30:37–84.
- Szyperski T, Antuch W, Schick M, Bets A, Stone SR, Wüthrich K. 1994. Transient hydrogen bonds identified on the surface of the NMR solution structure of hirudin. *Biochemistry* 33:9303–9310.
- Tanford C. 1968. Protein denaturation. *Adv Protein Chem* 23:121–281.
- Tanford C. 1970. Part C. Theoretical models for the mechanism of denaturation. *Adv Protein Chem* 24:1–95.
- Van Dael H, Haezebrouck P, Morozova L, Arico-Muendel C, Dobson CM. 1993. Partly folded state of equine lysozyme. Structural characterization and significance for protein folding. *Biochemistry* 32:11886–11894.
- Wu LC, Peng Z, Kim PS. 1995. Bipartite structure of the α -lactalbumin molten globule. *Nat Struct Biol* 2:281–286.
- Wu LC, Schulman BA, Peng Z, Kim PS. 1996. Disulfide determinants of calcium-induced packing in α -lactalbumin. *Biochemistry* 35:859–863.
- Yang A, Honig B. 1993. On the pH dependence of protein stability. *J Mol Biol* 237:459–474.